# Radiomic Analysis of the Instrumented Spinal Cord:
# A Post-Surgical Analysis of Degenerative Myelopathy and Acute Cord Injuries

Azadeh Sharafi[1], Andrew Klein[1], Kevin M Koch[1]
[1]Medical College of Wisconsin, Milwaukee, WI
asharafi@mcw.edu

**Disclosur**es: Authors have nothing to disclose.

**INTRODUCTION**:
Spinal Cord Injuries (SCI) and Cervical Spondylotic Myelopathy (CSM) are major health concerns, with SCIs affecting approximately 200,000 individuals worldwide annually and CSM being the prevalent cause of spinal dysfunction in older adults. Diagnostic imaging plays a pivotal role in assessing these injuries. Magnetic Resonance Imaging (MRI) is renowned for its exceptional cord and surrounding tissue visualization capabilities. However, despite its strengths, MRI can sometimes fall short in capturing the intricate microscopic or functional details of the spinal cord. Radiomics, which leverages image processing to derive metrics from conventional images, offers the potential for deeper tissue classification and improved diagnosis. However, post-surgical MRI images can have artifacts due to metallic hardware used in treatments like spinal fusion. This exploratory feasibility study seeks to develop pathology-specific diagnostic models using quantitative radiomic metrics of the damaged spinal cord in the immediate vicinity of fusion hardware using metal-artifact suppressed MRI.

**METHODS:**
Study Cohorts: The study evaluated 40 CSM patients' post-surgical decompression with metal spinal hardware, 12 sub-acute SCI subjects' post-surgery, and 50 controls, all above 18 years of age. All subjects provided written consent to an approved IRB protocol. Both CSM and SCI subjects had recent surgeries requiring metallic fusion stabilization hardware implantation. MRI Acquisition: Data was collected using a GE Signa Premier 3T scanner, capturing both T1 and T2-weighted 3D-MSI images. These images had an isotropic resolution of 1.2mm. Radiomic feature extraction: The algorithm initiated spinal cord segmentation in axial images using a semi-automatic method based on the open-source Spinal Cord Toolbox (SCT) [1], as detailed by Koch et al. [2]. First and second-order radiomics [3] were computed from axial cord segmentation sections after applying seven filters: wavelet, square, square root, logarithm, exponential, gradient, and local binary pattern. This process resulted in 1374 features per contrast per axial cord section. Classification targets: Using radiomics features, we assessed the differentiation between Control, CSM, and SCI groups. In the SCI group, we examined tissue characteristics relative to the injury site and grouped patients by their ASIA score into non-severe (A, B) and severe (C, D) categories. We further explored the radiomics' capacity to distinguish these categories. For the CSM group, we categorized zones as instrumented, adjacent to hardware, or normal and probed radiomics' ability to detect these zones. Additionally, we associated radiomics with myelopathy severity using MJOA scores.
Machine Learning: The H2O AutoML framework [4] was employed to find the best model for different classification targets. The dataset was split into training (70%), validation(15%), and testing(15%) subsets. The AutoML process generated up to 25 models, emphasizing class balance to avoid bias. A 5-fold cross-validation was used for evaluation, and the top-performing model was chosen based on log loss error.

**RESULTS:**
Figure 1 shows sample T1 and T2 weighted MRI images and the corresponding segmentation of an instrumented cord of an SCI and a CSM patient. Table 1 provides the modeling results. Performance against binary classification targets (2 categories) was highly successful for all tested models, with testing AUC values over 0.9 (i.e., severe SCI injury, CSM instrumented/adjacent segments, etc.). Multi-class modeling was less effective with higher classification errors. The best multi-class modeling was achieved in classifying control, SCI, and CSM cord tissues (class error of 0.15). The Gradient Boosting Model (GBM), XGBoost, and deep-learning grid (DLg) modeling approaches were the best performers.

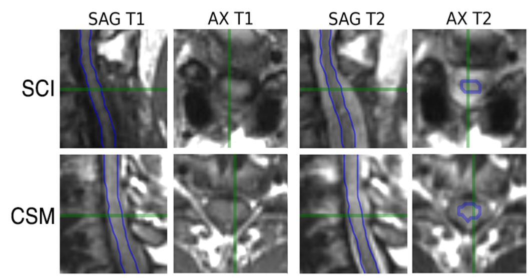


Figure 1. Representative 3D-MSI MRI images of SCI and CSM patients with fusion hardware employed for cord stenosis stabilization and treatment. Sagittal views: (a) T1-weighted and (c) T2-weighted. Axial reformats at the position indicated by the green line are shown in (b) and (d).

**DISCUSSION:**
This preliminary study has demonstrated the potential benefits of combining radiomics with machine learning in spinal cord diagnostics. Though strong performance was noted in cases of binary classifications, there was a marked increase in error rates during more complex, multinomial categorizations. This highlights two critical future needs: refining models for more complex cord tissue classifications and expanding the dataset to enhance accuracy.

**SIGNIFICANCE/CLINICAL RELEVANCE:**
The combination of radiomics feature generation and machine learning is helpful in researching and potentially categorizing spinal cord disorders, especially in post-surgical contexts. This enhanced diagnostic approach surpasses traditional MRI limitations, enabling a deeper understanding of spinal cord tissue characteristics, even amidst potential metallic hardware artifacts often used to treat spinal cord disorders. Expanding this capability could unlock tailored therapeutic strategies and monitoring of cord health.

Table 1. Comparative Performance Metrics of Machine Learning Models in Radiomic Classification of Spinal Cord Injuries and Myelopathy Severity.

| Dataset | Target | Cat. | model | logloss | RMSE | MSE | AUC |
|---|---|---|---|---|---|---|---|
| SCI | ASIA | 2 | GBM | 0.06 | 0.13 | 0.02 | 0.998 |
| CSM | MJOA | 3 | DLg | 0.08 | 0.22 | 0.05 | |
| All | Cohort & Lev | 7 | XGB | 0.21 | 0.31 | 0.10 | |
| All | Cohort | 3 | DLg | 1.38 | 0.37 | 0.14 | |
| SCI | Above Inj | 2 | GBM | 0.12 | 0.19 | 0.04 | 0.991 |
| SCI | Inj Lev | 2 | GBMg | 0.21 | 0.25 | 0.06 | 0.975 |
| SCI | Below Inj | 2 | GBM | 0.14 | 0.21 | 0.04 | 0.988 |
| SCI | Inj. Lev | 3 | XGBg | 0.09 | 0.25 | 0.06 | |
| CSM | Inst Lev. | 2 | GBMg | 0.14 | 0.20 | 0.04 | 0.989 |
| CSM | Adj Lev | 2 | GBMg | 0.37 | 0.35 | 0.12 | 0.921 |
| CSM | Inst/Adj Lev | 3 | XGB | 0.16 | 0.31 | 0.09 | |

**REFERENCES:**
1. De Leener, B., L´evy, S., Dupont, S.M., Fonov, V.S., et al. Sct: Spinal cord toolbox, an open-source software for processing spinal cord MRI data. Neuroimage 145, 24–43 (2017)
2. Koch, K.M., Nencka, A.S., Klein, A., Wang, M., et al. Diffusion-weighted mri of the spinal cord in cervical spondylotic myelopathy after instrumented fusion. Frontiers in Neurology 14, 1172833 (2023)
3. Griethuysen, J. J. M., Fedorov, A., Parmar, C., Hosny, A., et al., Computational Radiomics System to Decode the Radiographic Phenotype. Cancer Research, 77(21), e104–e107. (2017)
4. LeDell. E. and Poirier, S. H2O AutoML: Scalable Automatic Machine Learning. 7th ICML Workshop on Automated Machine Learning (AutoML), 2020

**ACKNOWLEDGEMENTS:** Funding provided by the Department of Defense Congressionally Directed Medical Research Program, Spinal Cord Injury Research Program, award number W81XWH1910273